

KSTAR Equilibrium Operating Space, H-mode Dynamics, and Projected Stabilization at High Normalized Beta*

**Y.S. Park¹, S.A. Sabbagh¹, J.W. Berkery¹, J.M. Bialek¹,
Y.M. Jeon², S.H. Hahn², J.K. Park³, N. Eidietis⁴,
T.E. Evans⁴, H. Park⁵, M. Walker⁴, J. Leuer⁴,
and KSTAR team**

¹Department of Applied Physics, Columbia University, New York, NY, USA

²National Fusion Research Institute, Daejeon, Korea

³Princeton Plasma Physics Laboratory, Princeton, NJ, USA

⁴General Atomics, San Diego, CA, USA

⁵POSTECH, Pohang, Korea

NSTX Monday Physics Meeting

March 14th, 2011

Collaborative research on KSTAR equilibrium and global MHD stability

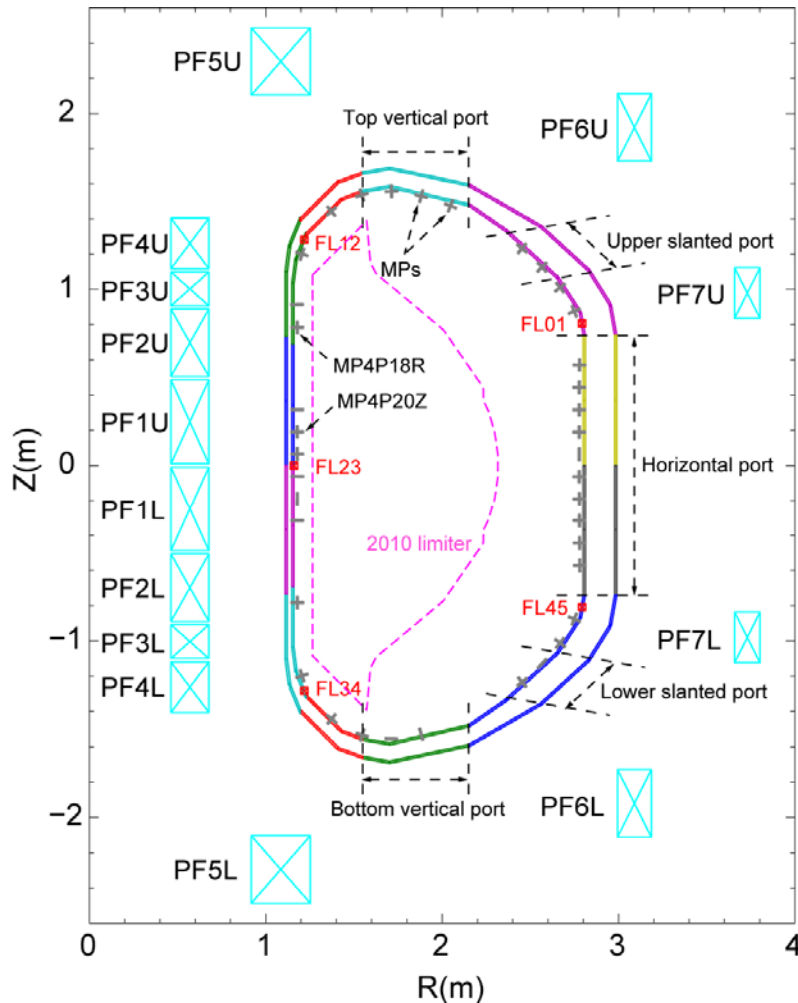
□ Scope of this collaborative research

- Support KSTAR experimental/theoretical equilibrium analysis
- Study on global MHD mode & rotation control physics for high beta operation regime
- Examine the edge localized mode (ELM) mitigation potential by resonant magnetic perturbations (RMP)

□ Research addressed in this talk

- Equilibrium reconstruction
 - EFIT code including theoretically estimated vessel current from VALEN-3D calculation
 - Equilibrium operating regimes of 2009 and 2010 KSTAR discharges
- Passive and active stabilization of resistive wall mode (RWM)
 - Kinetic modification of RWM stability by MISK calculation, which has been successfully used in NSTX
 - Passive stabilizing plate design to maximize RWM passive stabilization (finalized design applied to the passive stabilizing plates installed in 2010)
 - Power requirements for RWM active stabilization using IVCC including noise effect
- ELM suppression by RMP
 - TRIP3D calculations to evaluate vacuum island overlap created by RMP using a combination of all poloidal IVCC sectors with dominant $n = 2$ field spectrum
 - Appropriate RMP condition for 2011 XP in terms of coil parity and q -profile

EFIT model for reconstruction of 2009-10 KSTAR discharges



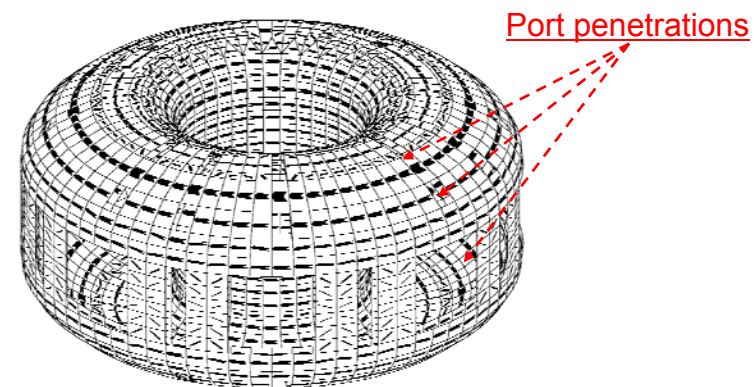
KSTAR configuration used in equilibrium reconstruction (12 vessel current groups are indicated by regions of different colors)

EFIT setup/input

- 14 PF currents, 67 (57) magnetic probes, 5 flux loop voltage monitors, 0 (5) flux loops, 1 Rogowski coil are used as constraints
**Numbers in parenthesis are for 2010 reconstruction*
- Simple plasma basis function model is used for reliable reconstruction with lack of internal measurements

Vessel current estimation in EFIT

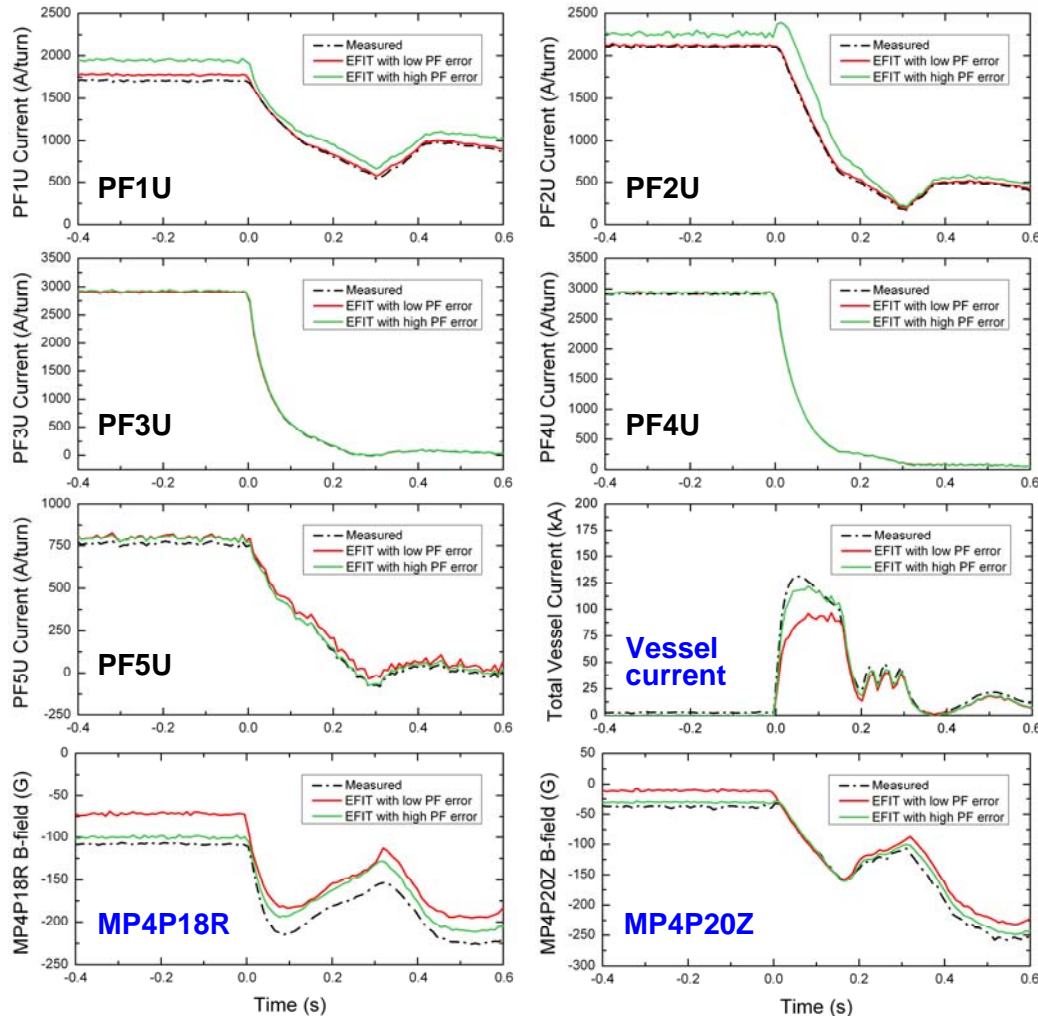
- Vessel current is represented as 12 independent current carrying groups
- Effective vessel group resistances from a VALEN-3D code startup calculation are used to estimate vessel currents



Vessel currents in VALEN-3D startup calculation

Allowance for ferromagnetic Incoloy effect in reconstruction

EFIT vacuum field reconstruction for shot 1845 by using different PF errors
(low error : $\sigma_{rel} = 0.5\%$, high error : as shown in table below)



❑ Incoloy materials in KSTAR coils

- ❑ Conduit conductor of TF and some of PF coils (PF1-5) include ferromagnetic Incoloy material (magnetic permeability ≈ 10)
- ❑ Magnetic nonlinearity causes certain inconsistencies between measured and reconstructed signals

❑ Increased PF error reasonably allows for Incoloy effect

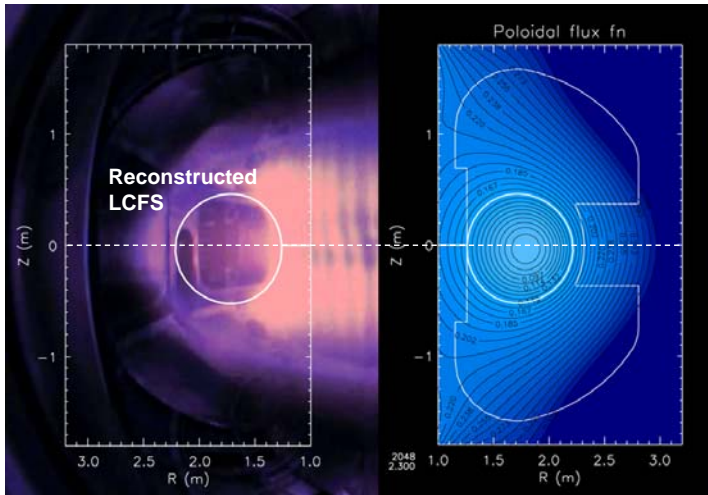
- ❑ PF1-2 are found to carry most of the compensating currents
- ❑ The discrepancies in vessel current and MPs are mostly balanced by this change

PF1UL	PF2UL	PF3UL	PF4UL	PF5UL	PF6UL	PF7UL
8%	10%	4%	3%	1.5%	1%	1%

Relative errors set on PF coils for reasonable allowance for paramagnetic Incoloy effect

Reconstruction result: shot 2048 reached maximum W_{tot} in 2009

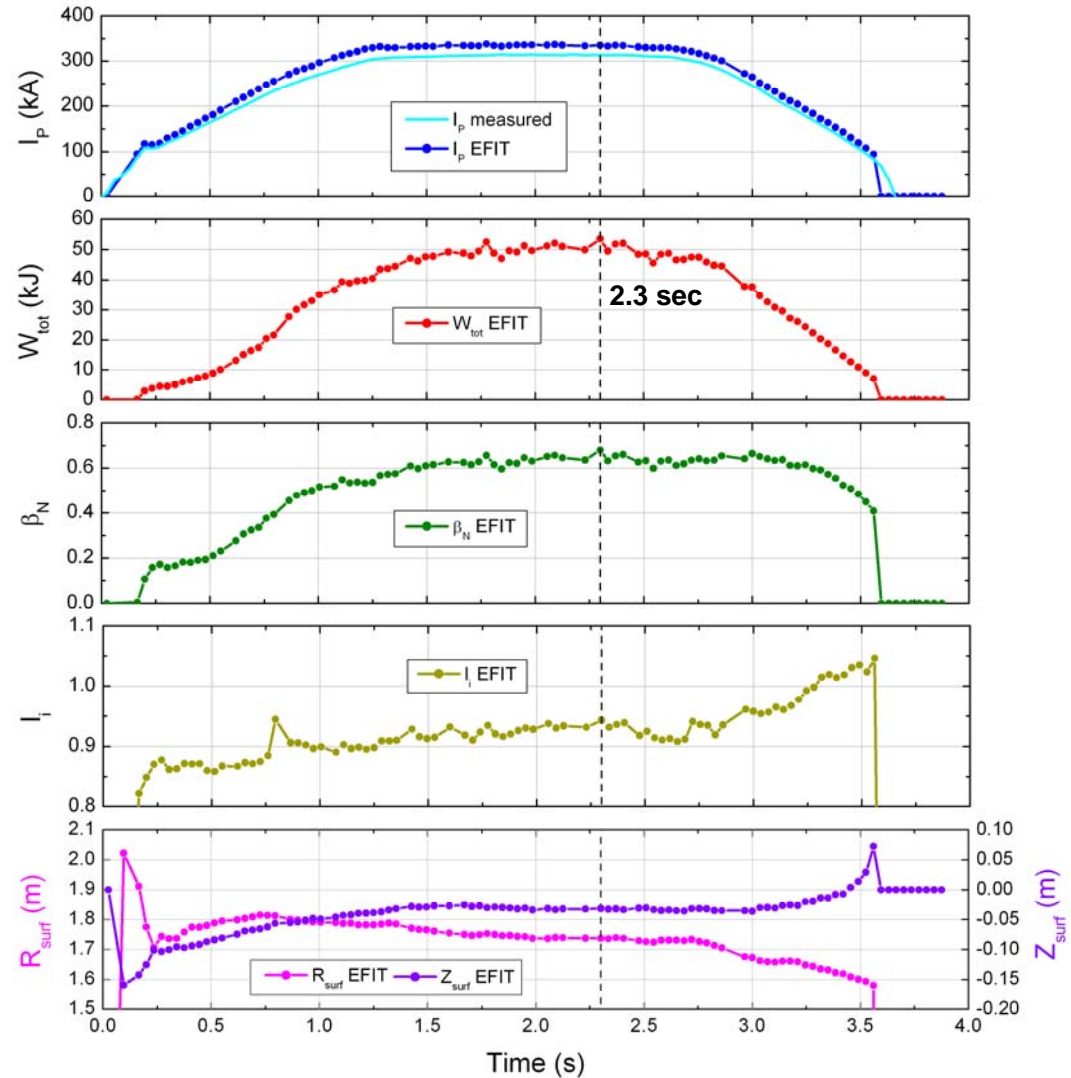
- Shot 2048 reached plasma stored energy, $W_{tot} = 54$ kJ, which is the maximum value among the 2009 discharges



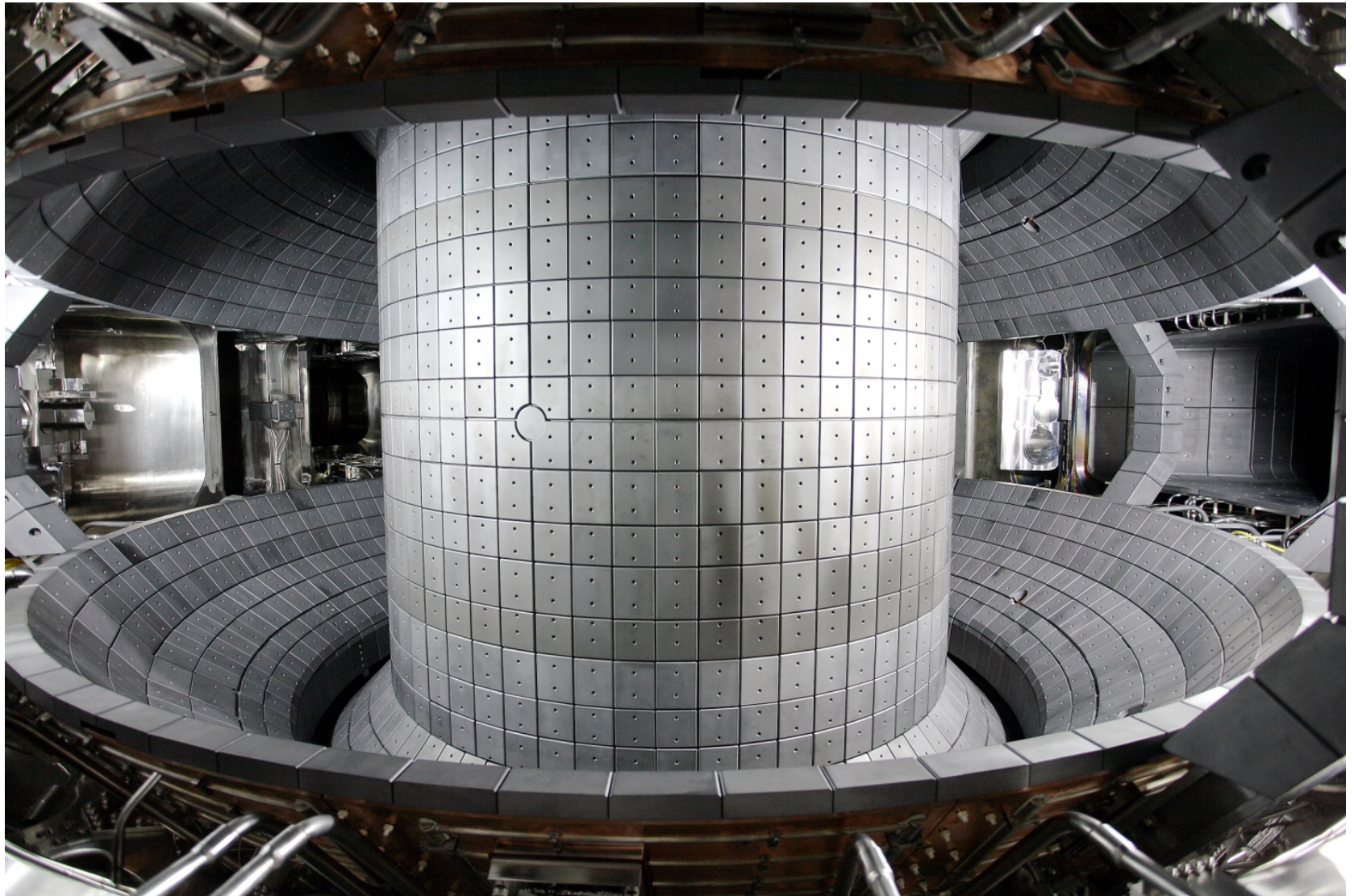
Fast framing camera image and reconstructed equilibrium flux surfaces at $t = 2.3$ sec for shot 2048

- Plasma is downshifted in most of the reconstructed equilibria, which may due to additional current flowing in the bottom of cryostat (S.W. Yoon, IAEA 2010, EXS/5-1)

Evolution of reconstructed plasma parameters in shot 2048

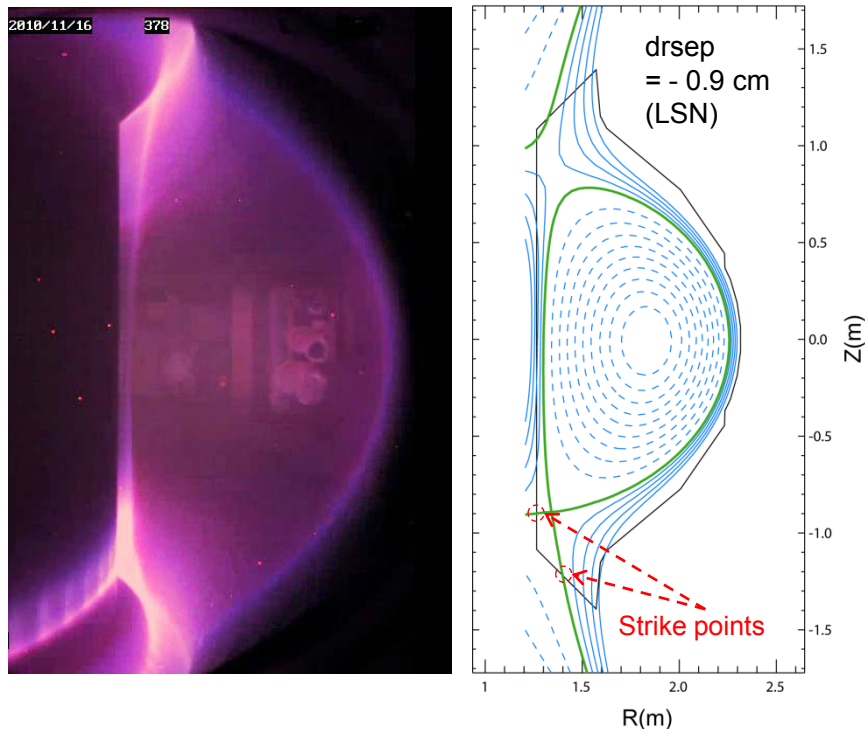


View of KSTAR in-vessel structure completed in 2010

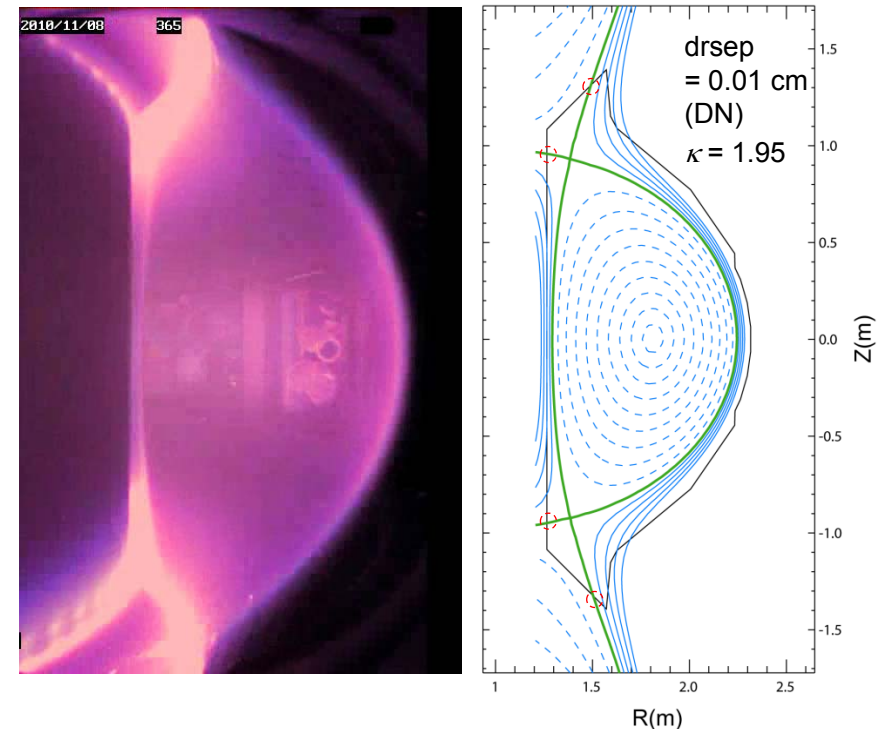


Equilibrium configurations were mostly LSN in 2010

- Equilibria in 2010 were mostly in LSN configuration and DN was transiently achieved during vertical movement of plasma
- Reconstructed boundaries from EFIT are very consistent with fast camera image



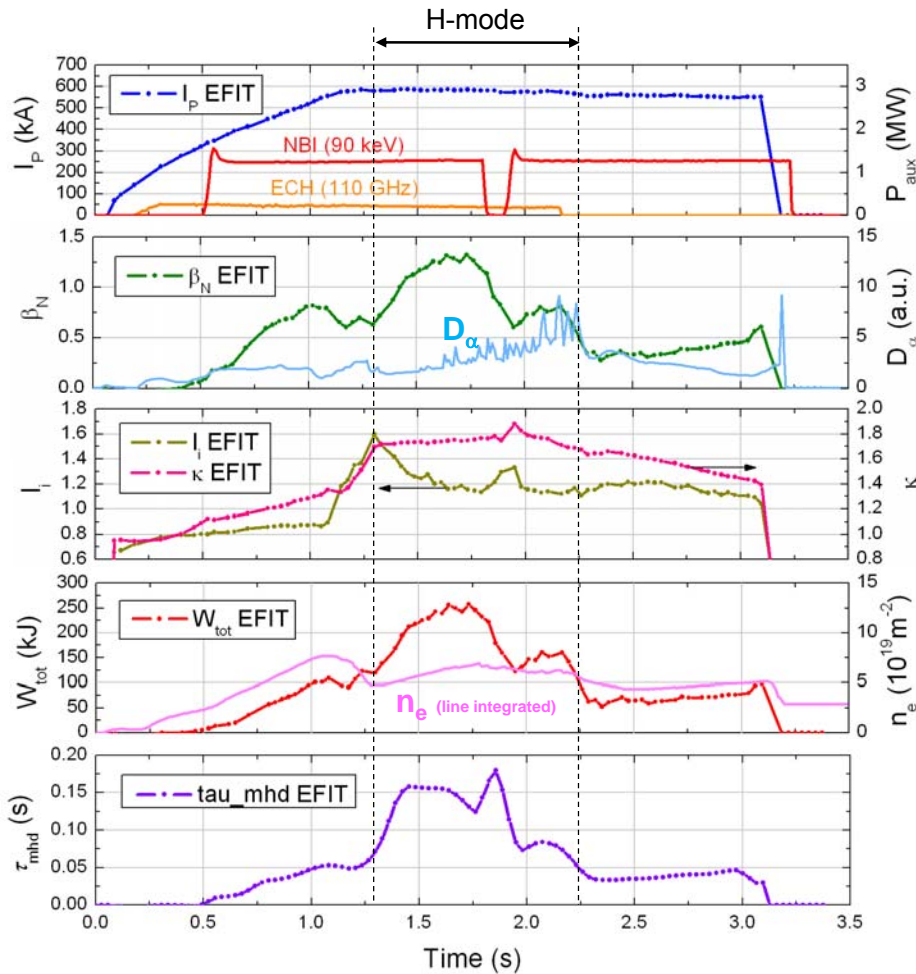
Fast framing camera image and reconstructed equilibrium flux surfaces at $t = 1.73$ sec for shot 4358 (time of maximum W_{tot} in 2010)



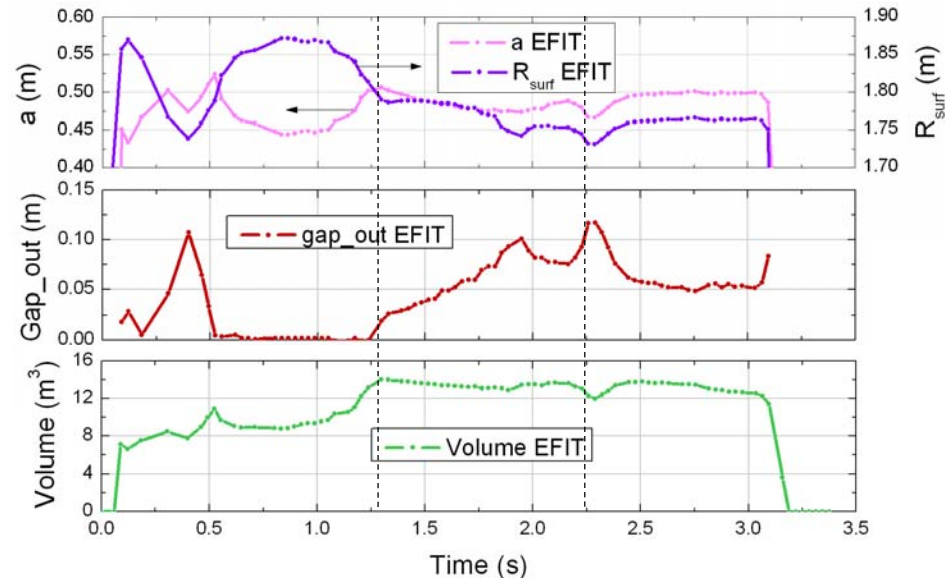
Fast framing camera image and reconstructed equilibrium flux surfaces at $t = 1.66$ sec for shot 4202 (time of maximum transient κ in 2010)

Reconstruction of H-mode discharges in 2010

- Shot 4358 reached plasma stored energy, $W_{tot} = 258$ kJ and normalized beta, $\beta_N = 1.34$ which are the maximum values among the 2010 discharges



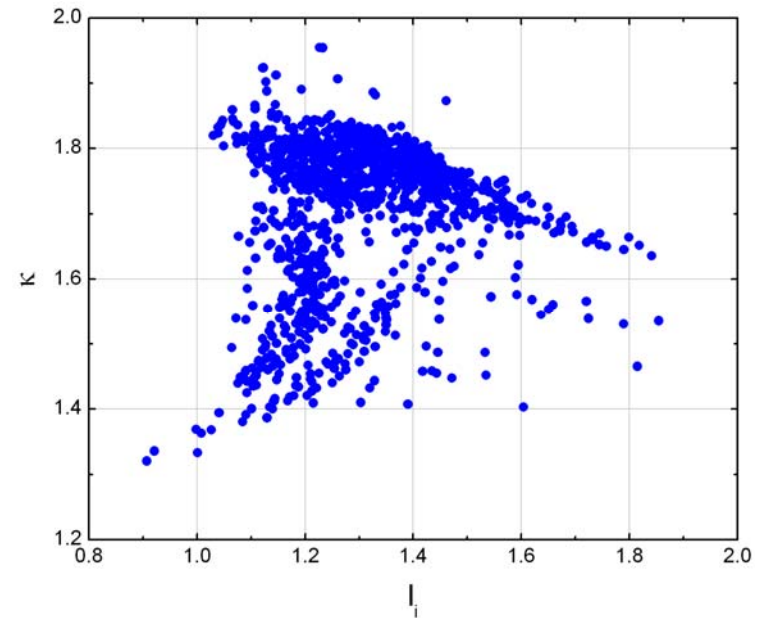
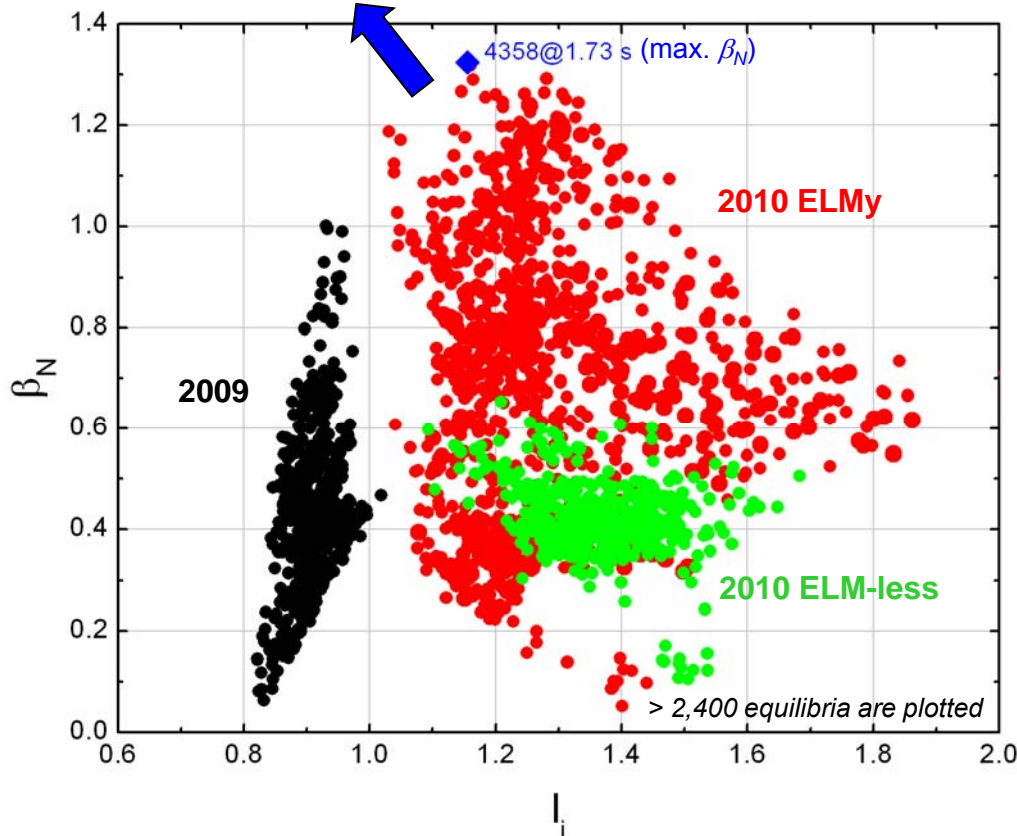
$$\tau_E \text{ (at max } W_{tot}) = 148 \text{ msec, } \tau_E^{MAX} = 163 \text{ msec}$$



Evolution of reconstructed plasma parameters in shot 4358

Equilibrium operating space of 2009-10 discharges

2011 XP



Plasma elongation vs. internal inductance of elongated equilibria in 2010 (27 shots)

Equilibrium operating regime drawn in (I_i, β_N) space explored by 2009-10 discharges

- black : 2009 ohmic circular discharges (18 shots)
- red : 2010 ELMy H-mode discharges (24 shots)
- green : 2010 ELM-less discharges (9 shots)

Summary of equilibrium records for 2009-10 discharges

2009 near-circular,
ohmic discharges

Shot number

	2136	2074	2048	1924	2155
I_p	361 kA	285 kA	337 kA	139 kA	290 kA
β_N	0.62	0.99*	0.73	0.32	0.68
l_i	0.84	0.92	0.89	0.84	0.85
W_{tot}	48 kJ	44 kJ	54 kJ	9.5 kJ	35 kJ
κ	1.04	1.03	1.03	1.08	1.03
t_{pulse}	3.69 s	3.63 s	3.62 s	1.50 s	4.05 s



2010 elongated,
beam-driven discharges

	4340	4358	4202	4445
I_p	693 kA	587 kA	575 kA	332 kA
β_N	0.44	1.34	1.09	0.41
l_i	1.02	1.11	1.10	1.18
W_{tot}	72 kJ	258 kJ	228 kJ	63 kJ
κ	1.83	1.79	1.85	1.78
t_{pulse}	3.62 s	3.21 s	1.83 s	6.69 s

Those are representative values during current flattop. *The higher β_N of shot 2074 is due to the steady I_p decrease around $t = 2.3$ s.

Kinetic stabilization of RWM in KSTAR being analyzed using a physics model successfully used in NSTX

- ❑ Simple critical ω_ϕ threshold stability models do not describe experimental marginal stability (window of ω_ϕ with weakened stability exists)
- ❑ Kinetic effects modify ideal MHD $n = 1$ stability
 - ❑ Trapped and circulating ions, trapped electrons
 - ❑ Alfvén dissipation at rational surfaces

$$(\gamma - i\omega_r)\tau_w = -\frac{\delta W_\infty + \delta W_K}{\delta W_b + \delta W_K}$$

kinetic modification

Trapped ion component (typically accounts for 70~80% of $\text{Re}(\delta W_K)$)

$$\delta W_K \propto \int \left[\frac{\omega_{*N} + \left(\hat{\varepsilon} - \frac{3}{2}\right)\omega_{*T} + \omega_E - \omega - i\gamma}{\langle \omega_D \rangle + l\omega_b - i\nu_{eff} + \omega_E - \omega - i\gamma} \right] \hat{\varepsilon}^{\frac{5}{2}} e^{-\hat{\varepsilon}} d\hat{\varepsilon}$$

where, $\omega_E = \omega_\phi - \omega_{*i}$

ion diamagnetic frequency

precession drift bounce collisionality EXB

B. Hu, PRL **93** (2004) 105002
 J.W. Berkery, PRL **104** (2010) 035003
 S.A. Sabbagh, NF **50** (2010) 025020

- ❑ Stability modification depends on
 - ❑ Integrated ω_ϕ profile: resonances in δW_K (e.g. ion precession drifts)
 - ❑ Particle collisionality
- ❑ Plasma is stable when rotation is in resonance
 - ❑ $l = 0$ harmonic : resonance with precession drift frequency
 - ❑ $l = -1$ harmonic : resonance with bounce frequency

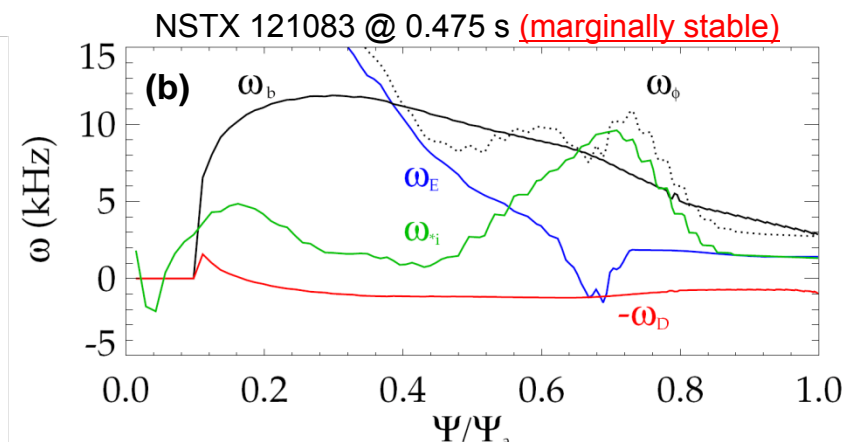
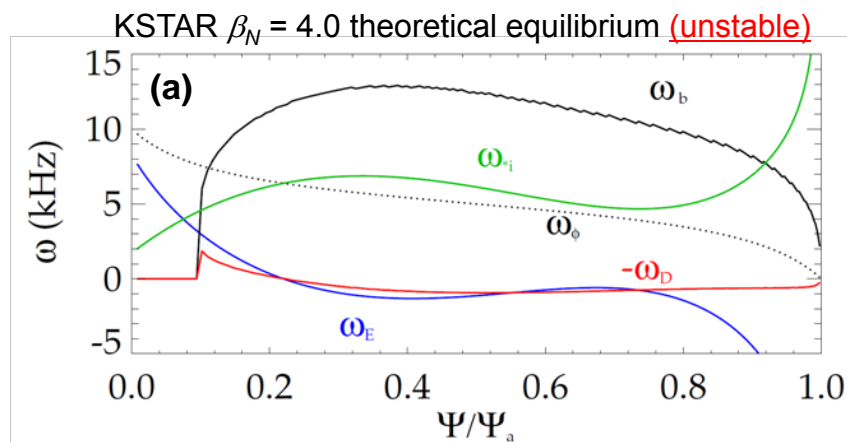
$$\omega_E + \langle \omega_D \rangle = 0$$

$$\omega_E - \omega_b = 0$$

key resonances

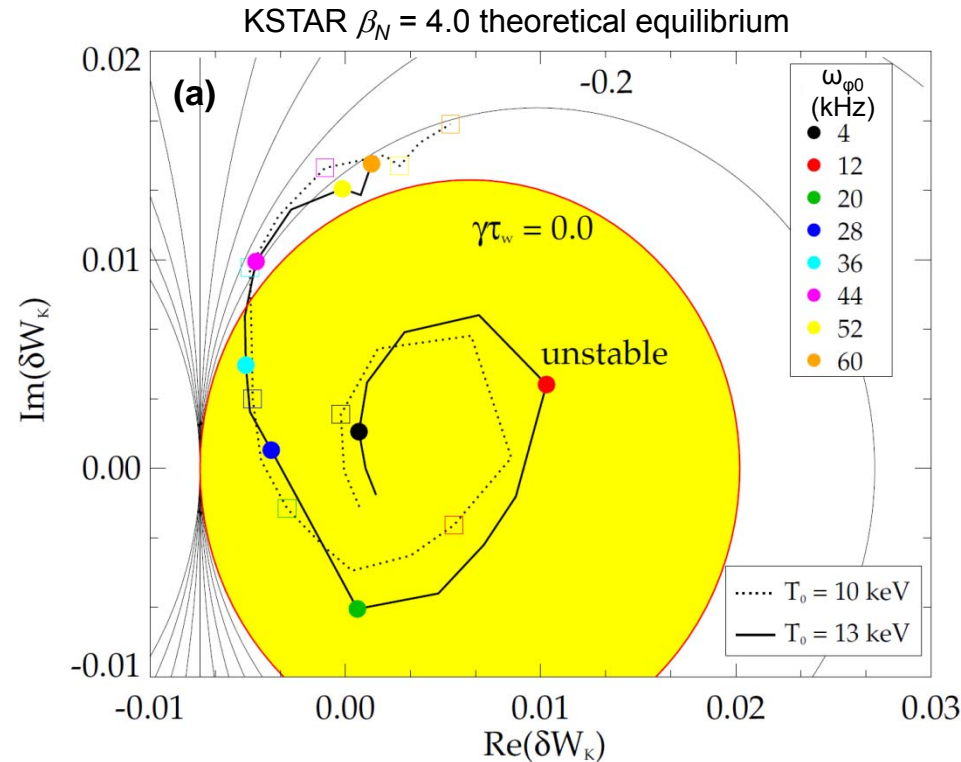
MISK calculation for KSTAR theoretical equilibrium

- ❑ MISK (Modification of Ideal Stability by Kinetic theory) code is used to calculate kinetic modification of RWM stability in KSTAR
- ❑ Target KSTAR equilibrium:
 - ❑ A theoretical equilibrium with $\beta_N = 4.0$, $l_i = 0.7$ and H-mode pressure profile ($n_e = n_i$, $T_e = T_i$)
 - ❑ Rotation profile similar to NSTX (all co-directed beams)
- ❑ Results:
 - ❑ The steep edge gradient of the target equilibrium causes a large ion diamagnetic frequency and a large negative ExB frequency near the edge
 - ❑ For the chosen profile ($\omega_{\phi 0} = 10$ kHz), the trapped thermal ion precession drift resonance is insufficient in the outer surface where the RWM eigenfunction is large



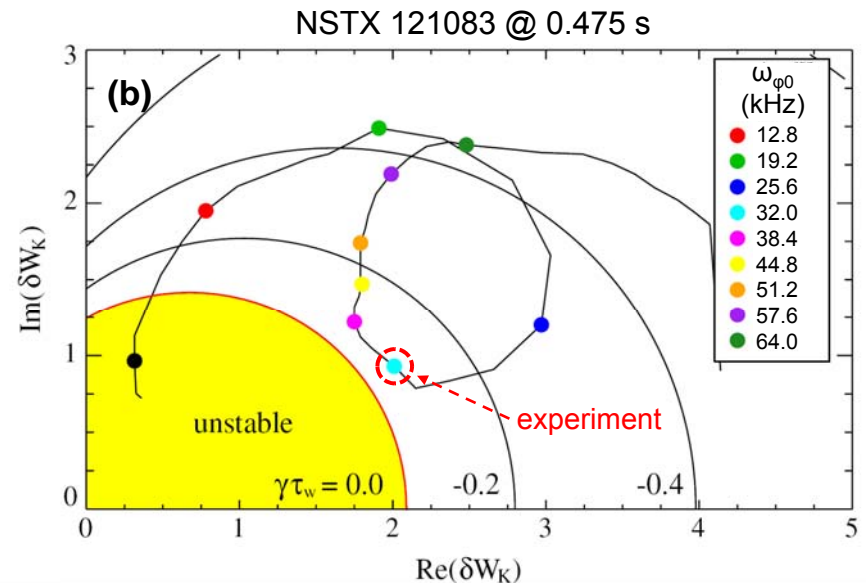
(a) Profiles of $\omega_{\phi 0}$, $\omega_{i 0}$, the resulting ω_E , and ω_b and $-\omega_D$ with zero pitch angle and $\varepsilon/T = 2$ and $3/2$, respectively (b) similar profiles from NSTX shot 121083 at $t = 0.474$ s where RWM is marginally stable

RWM stability diagrams for KSTAR and NSTX



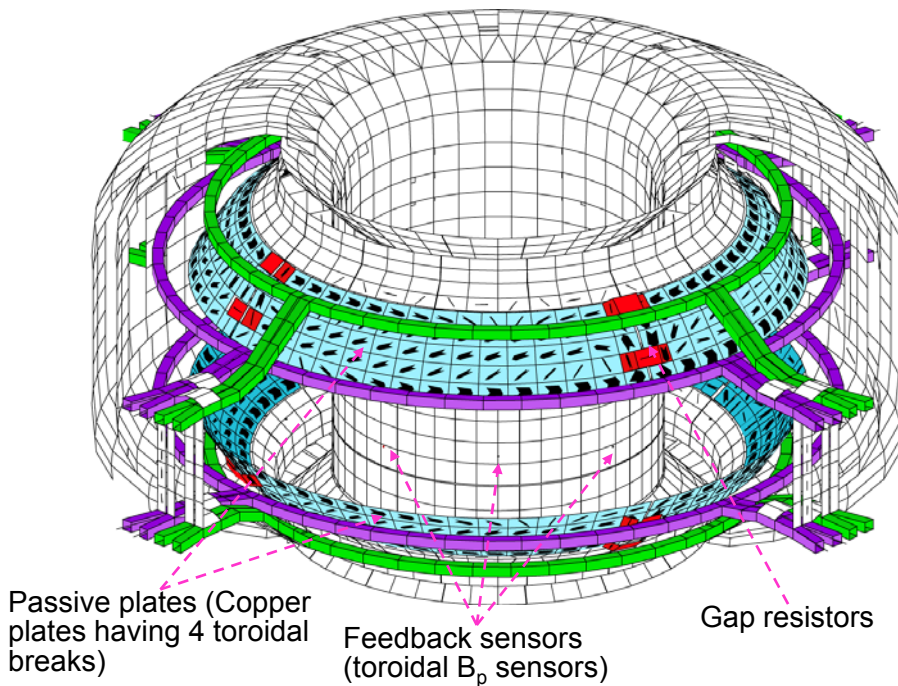
(a) Stability diagram for theoretical $\beta_N = 4.0$ KSTAR equilibrium with varied rotation profiles with $\omega_{\phi 0}$ from 0~60 kHz and (b) for NSTX shot 121083 at $t = 0.475$ s. The experimental point labeled “32.0” is close to marginal stability

- Stability diagram: contours of constant $\gamma\tau_w$ for varying rotation profile magnitude
- Compared to NSTX, KSTAR requires higher rotation for kinetic stabilization of RWM
 - Due to the lack of resonance in the outer region of the plasma, relatively large rotation $\omega_{\phi 0} \sim 42$ kHz is required for stability with $T_0 = 13$ keV, $n_0 = 1.3 \times 10^{20} \text{ m}^{-3}$ and $\omega_{\phi 0} \sim 34$ kHz with $T_0 = 10$ keV, $n_0 = 1.7 \times 10^{20} \text{ m}^{-3}$

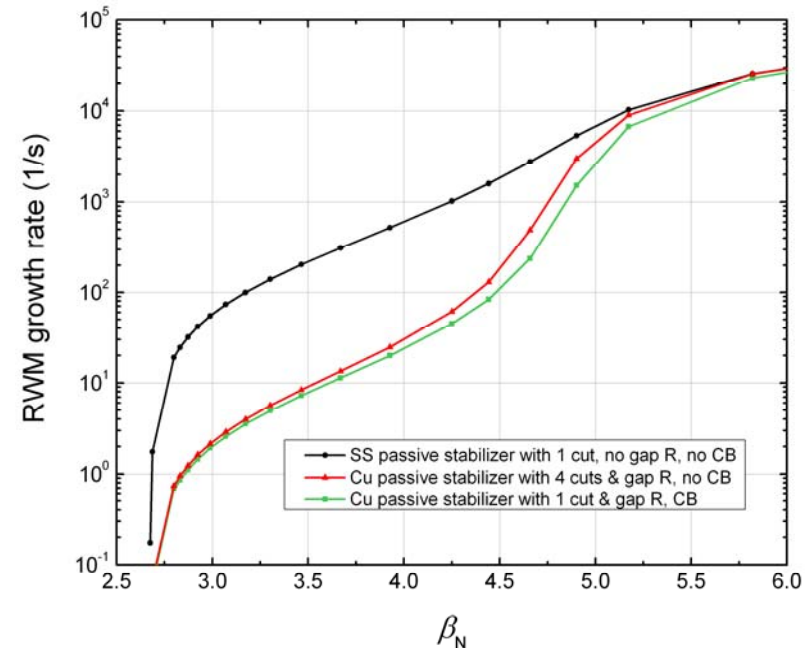


KSTAR passive stabilizing plate design was finalized to maximize RWM passive stabilization

- ❑ Passive stabilizing plate design was finalized and installed in 2010 after considering the impact of materials (SS vs. Cu) and electrical connections on RWM growth rates
 - ❑ The final design utilizes Cu plates, each having 4 toroidal high resistance breaks and current bridges were eliminated due to the increased potential for error fields
 - ❑ Copper plates reduce the RWM growth rate by a factor of 15 compared to SS at $\beta_N = 4.5$



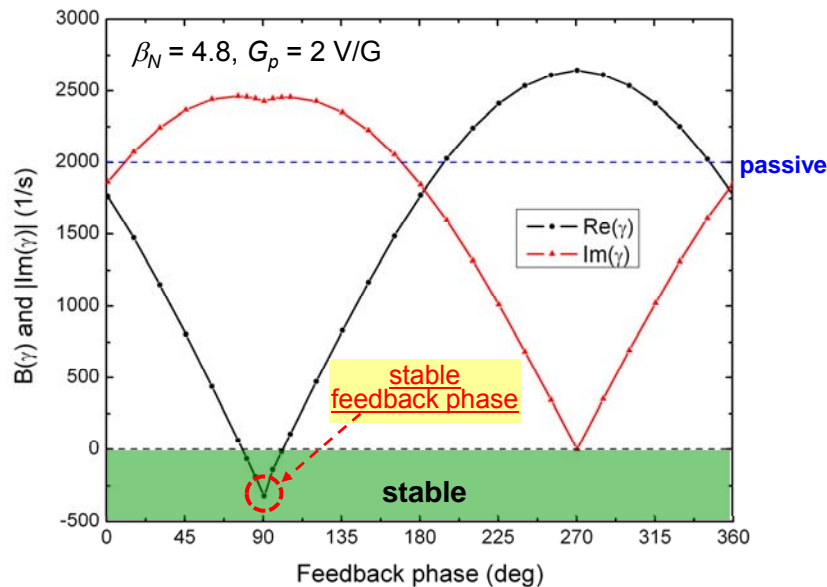
KSTAR conducting structure and IVCC (top, middle, bottom FECs) with surrounding conductive casing in VALEN model



RWM growth rate vs. β_N with different passive plate options: (i) SS, 1 toroidal cut (black), (ii) Cu, 1 toroidal cut and current bridge (green), (iii) Cu, 4 toroidal cuts (red)

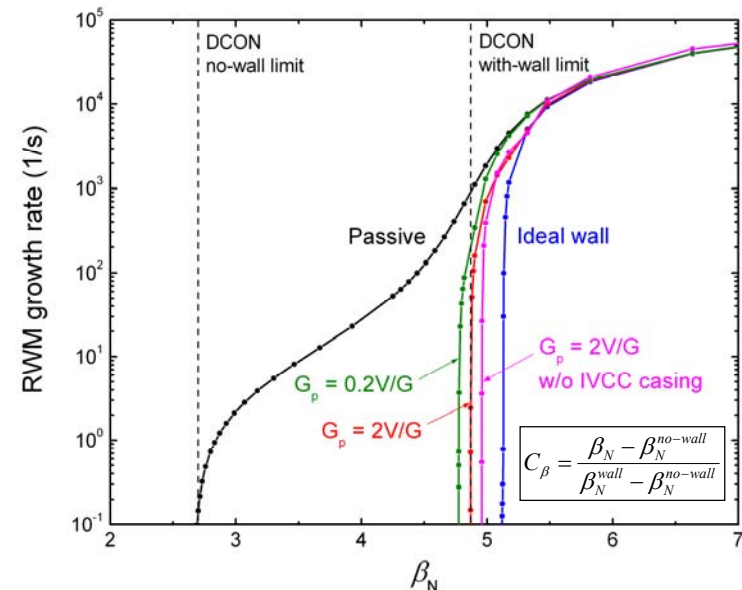
RWM feedback phase scan and resulting mode growth rate with different feedback gains

- Unstable $n = 1$ eigenfunction from DCON for a theoretical equilibrium with $\beta_N = 5.0$, $l_i = 0.7$ and H-mode pressure profile is used in VALEN code growth rate calculations
- Middle-FEC coil with SS casing is used for RWM active stabilization



Variation of real and imaginary values of growth rate which denote amplitude and rotation of the mode, respectively vs. feedback phase

- A stable feedback phase between B_p sensor set and control coil voltages is found

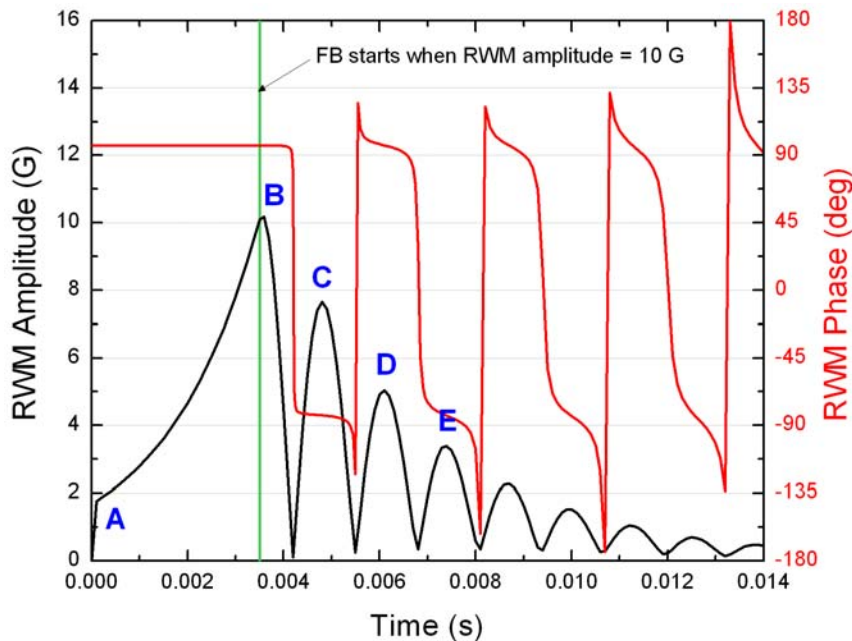


Mode growth rate vs. β_N with different feedback gains

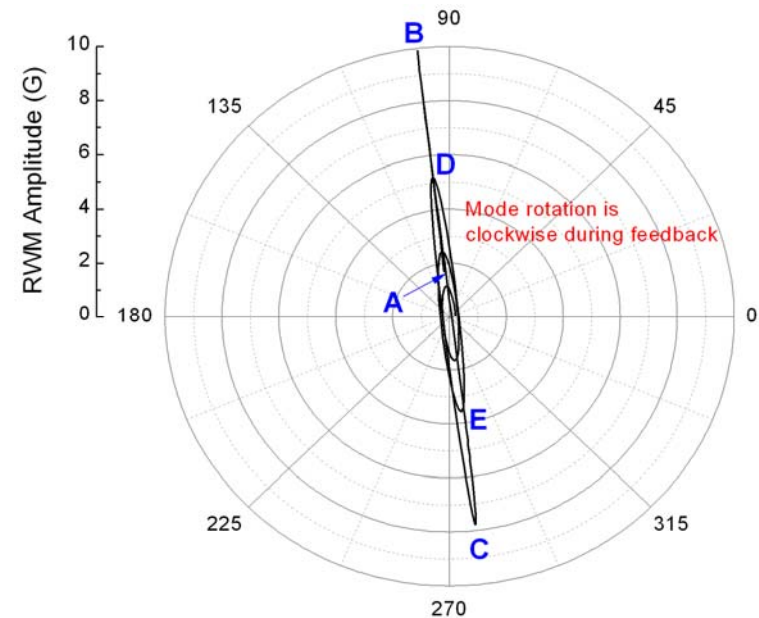
- Plasma can be stabilized up to with-wall limit ($C_\beta = 99\%$) predicted by DCON with controller gain $G_p = 2 \text{ V/G}$ and stable FB phase
- Conductive casing of IVCC shows a small degradation of control performance, which results in the reduction of C_β by $\sim 5\%$

Time domain RWM active stabilization calculation for stable feedback phase

- ❑ Ideal control system without noise or time delay is assumed
- ❑ Stable feedback phase is used for an equilibrium having $\beta_N = 4.8$ ($C_\beta = 98\%$) with $G_p = 2$ V/G
- ❑ Feedback starts when mode amplitude becomes 10 G
- ❑ RWM amplitude becomes less than 1 G and mode rotation is clockwise during feedback



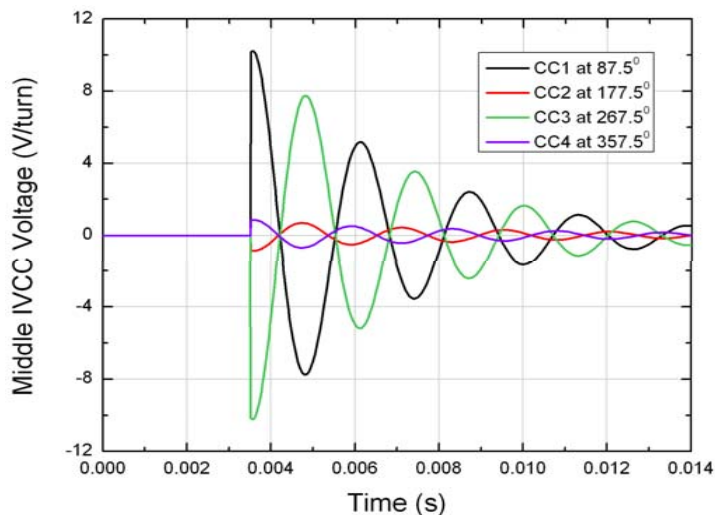
RWM amplitude and phase during feedback stabilization with stable feedback phase



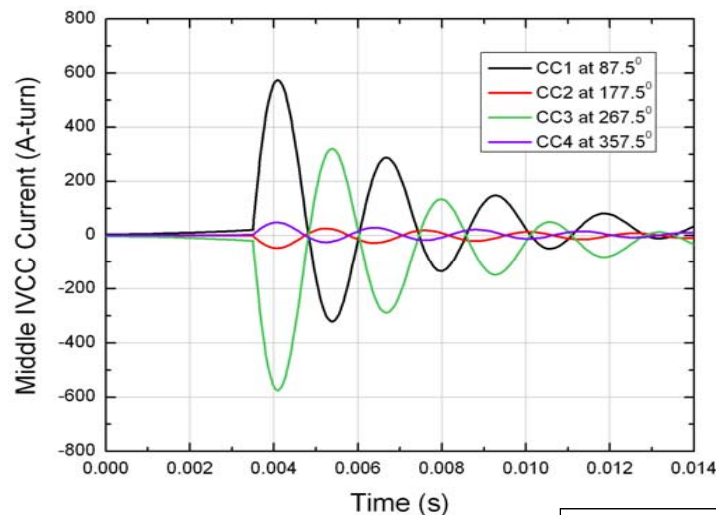
Polar plot of RWM behavior during feedback

Ideal power requirements for RWM active stabilization

Control coil voltage (unloaded circuit)



Control coil current (unloaded circuit)



Summary of middle-IVCC power requirements at $C_\beta = 98\%$ with $G_p = 2$ V/G

Unloaded circuit

$L = 44 \mu\text{H}$
 $R = 3.66 \text{ m}\Omega$
 $L/R = 12 \text{ ms}$



	CC1 @ 87.5°	CC2 @ 177.5°	CC3 @ 267.5°	CC4 @ 357.5°
I_{RMS} (A)	96.2	8.8	96.2	8.8
V_{RMS} (V)	1.59	0.16	1.59	0.16
P_{RMS} (W)	412.5	3.03	412.6	3.04

RMS time interval:
 20 x RWM growth times
 = 39 msec

Total RMS power:
0.83 kW

Fast circuit (loaded)

$L = 44 \mu\text{H}$
 $R = 44 \text{ m}\Omega$
 $L/R = 1 \text{ ms}$



	CC1 @ 87.5°	CC2 @ 177.5°	CC3 @ 267.5°	CC4 @ 357.5°
I_{RMS} (A)	72.2	7.0	72.2	7.0
V_{RMS} (V)	1.24	0.12	1.24	0.12
P_{RMS} (W)	387.5	3.7	387.5	3.7

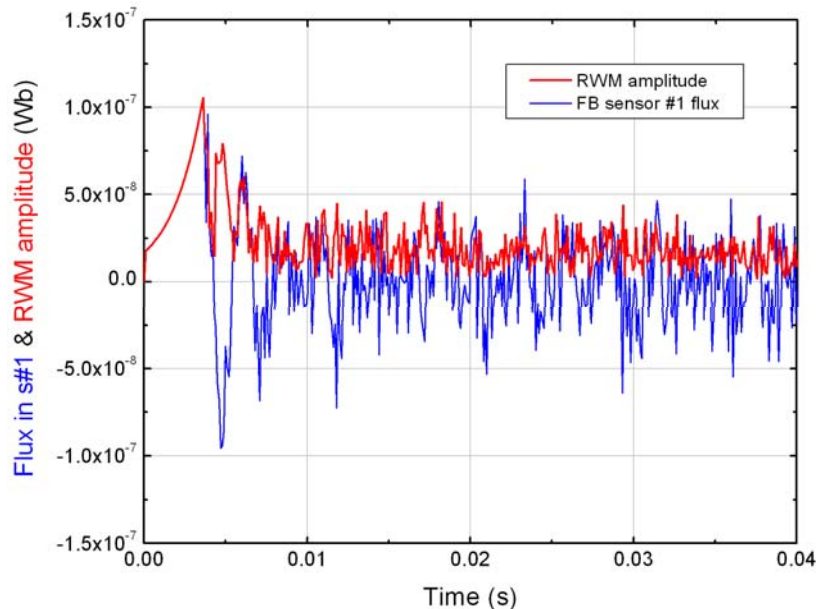
Total RMS power:
0.78 kW

Required feedback control power increases due to sensor noise, but remains at reasonable levels

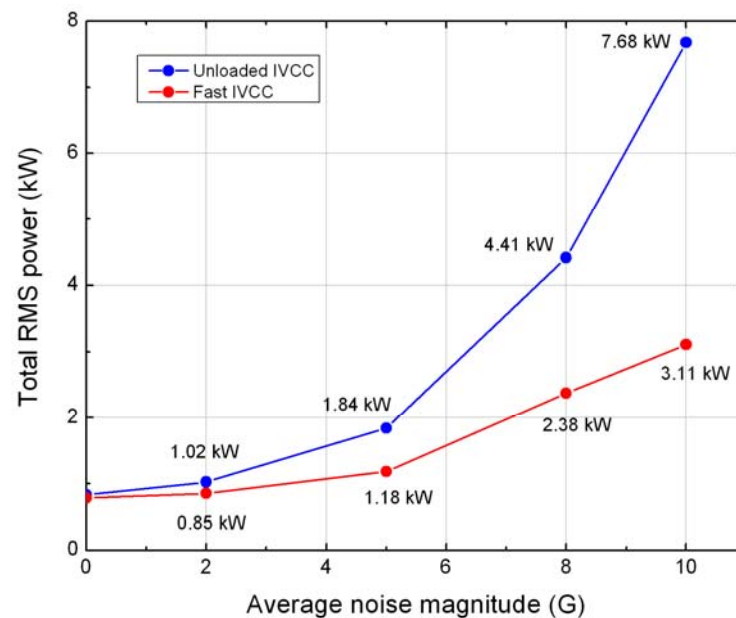
□ Approach

- Allow passive growth of RWM to 10 G then start feedback with 10 kHz, 2 ~ 10 G white noise in mode detection sensors (8 midplane B_p sensors)
- Same RMS time interval: 20 x RWM growth times = 39 msec

RWM amplitude & sensor flux with noise



Total RMS power of IVCC vs. sensor noise level



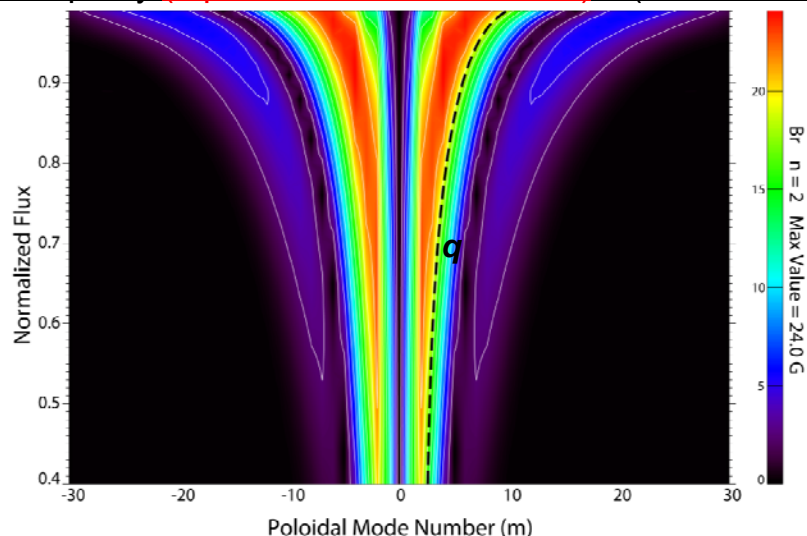
- *Unloaded IVCC with 2 G white noise*
- *Feedback & noise start when mode becomes 10 G*

- *Direct experience of PS needs from NSTX and DIII-D*
- *Presently a key consideration for $n = 1$ feedback in ITER*

Potential for ELM mitigation by RMP from IVCC: Even parity is more favorable for resonance pitch alignment

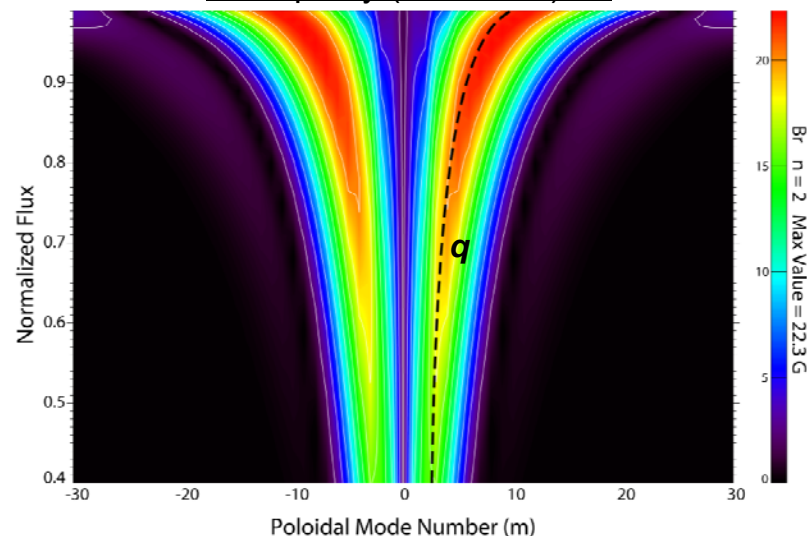
- ❑ The TRIP3D code is used to calculate RMP spectrum pitch alignment with a theoretical equilibrium having $q_{95} = 3.6$ and $\beta_N = 2.5$ with an experimental H-mode pressure profile
- ❑ A combination of all poloidal IVCC sectors (top, middle, bottom IVCCs) is used

Odd parity (top, middle, bottom IVCCs) = (+12, 0, -12) kA



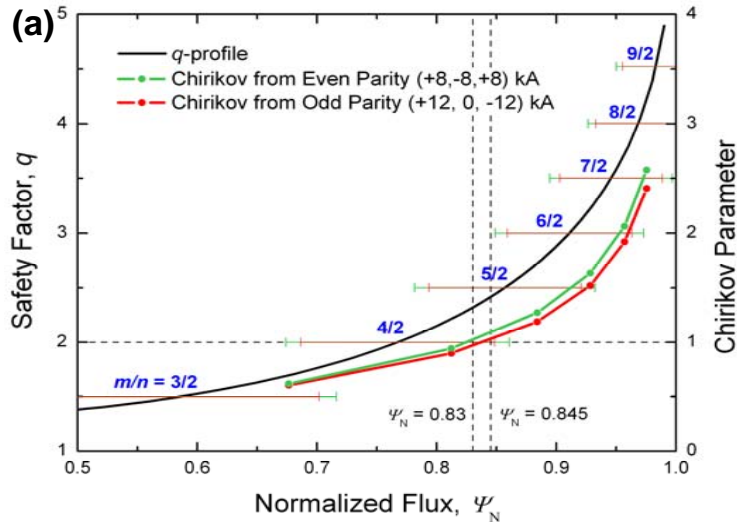
- ❑ Odd parity has relatively lower m -spectrum caused by utilizing only 2 poloidal IVCC sectors
- ❑ The perturbation is not efficiently coupled to q -profile and perturbs more into the core

Even parity (+8, -8, +8) kA

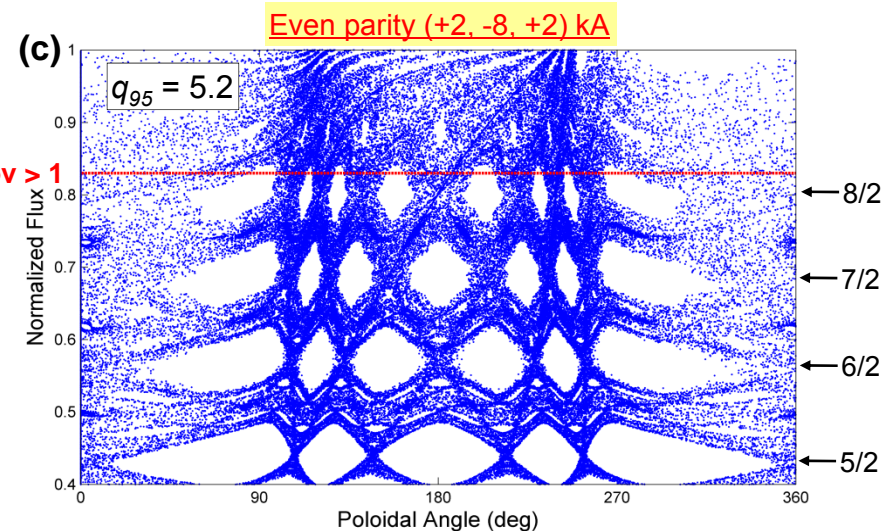
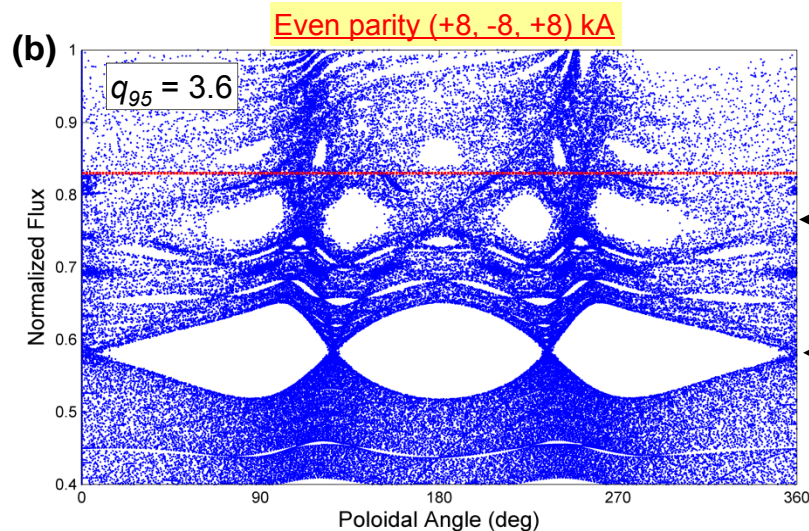


- ❑ Resonant field spectrum is localized around the plasma edge, higher m -spectrum aligns better with q -profile
- ❑ The amount of middle-FEC current can change the applied m -spectrum
- ❑ Favorable to make a pitch alignment with elevated q -profiles

Island overlap created by the odd and even parity RMPs



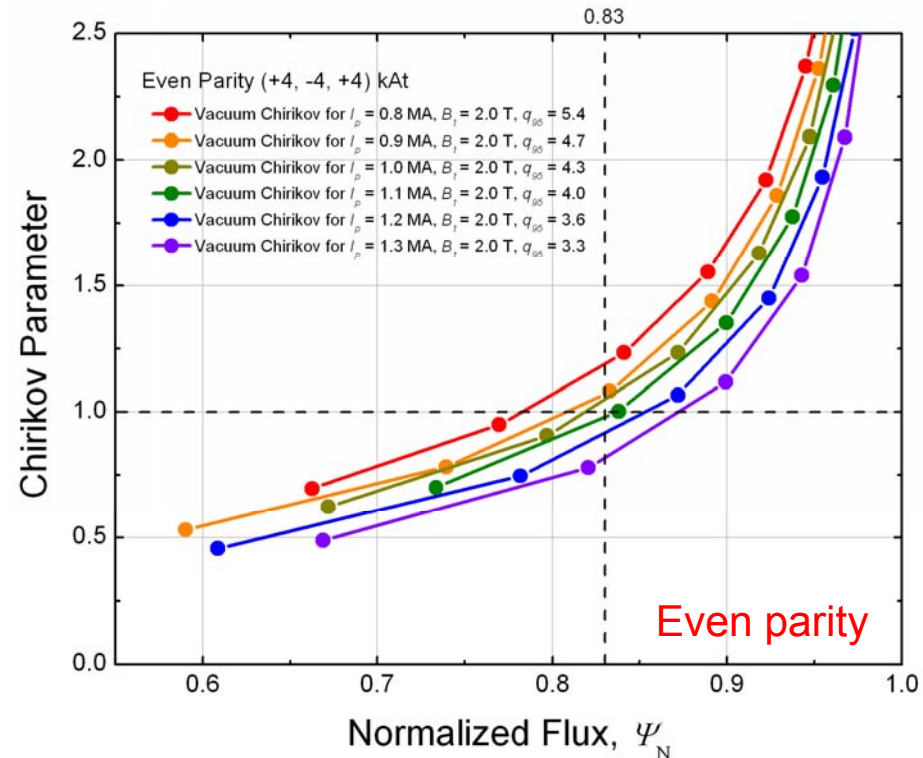
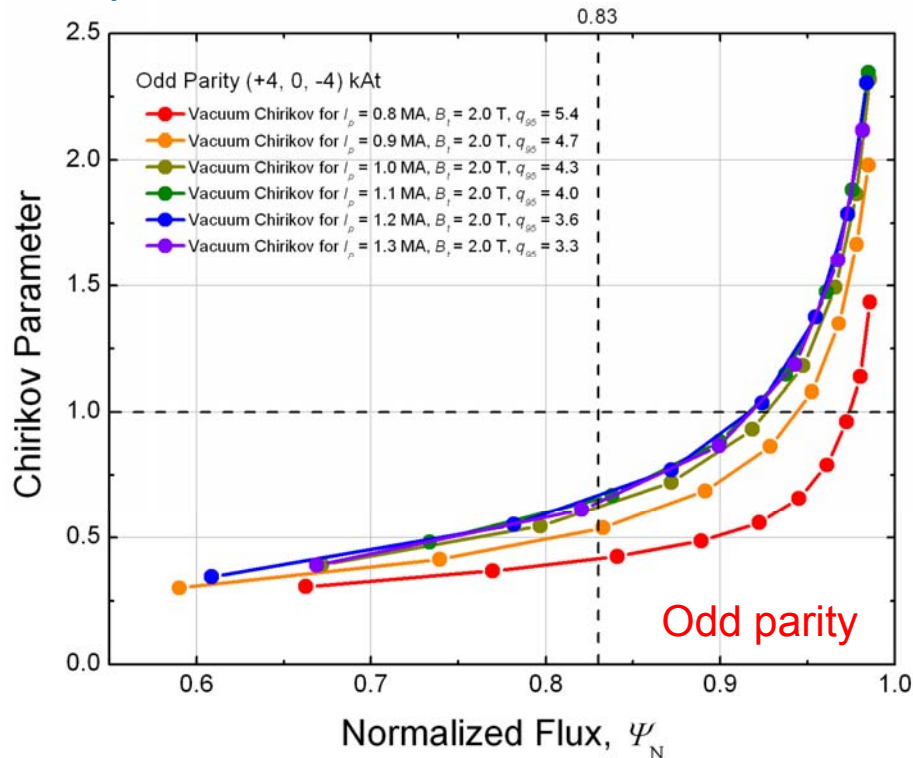
- Island widths are larger in even parity than those in odd parity due to better pitch alignment with a ridge in the resonant field spectra
- In the even parity, Chirikov parameter > 1 from $\Psi_N = 0.83$ which is empirically determined ELM mitigation condition in DIII-D (M.E. Fenstermacher, PoP 15 (2008) 056122), and the odd parity creates the condition at higher Ψ_N
- Even parity can fulfill the same Chirikov condition by using much smaller total current for equilibria having elevated q -profile



(a) Vacuum Chirikov profiles and $n = 2$ resonant harmonic island widths from the odd and even parity cases
 (b) Poincare plot using even parity for an equilibrium having $q_{95} = 3.6$, $\beta_N = 2.5$ and (c) $q_{95} = 5.2$, $\beta_N = 4.0$

Even parity fulfills the vacuum Chirikov criterion for equilibria expected in 2011 XP

- Use theoretical equilibria having $B_T = 2.0$ T, $\beta_N = 1.5$, $I_i = 1.0$ with different I_p to vary the q -profile
- The maximum allowable currents in 2011 XP (4 kAt) are applied to all poloidal IVCC sectors



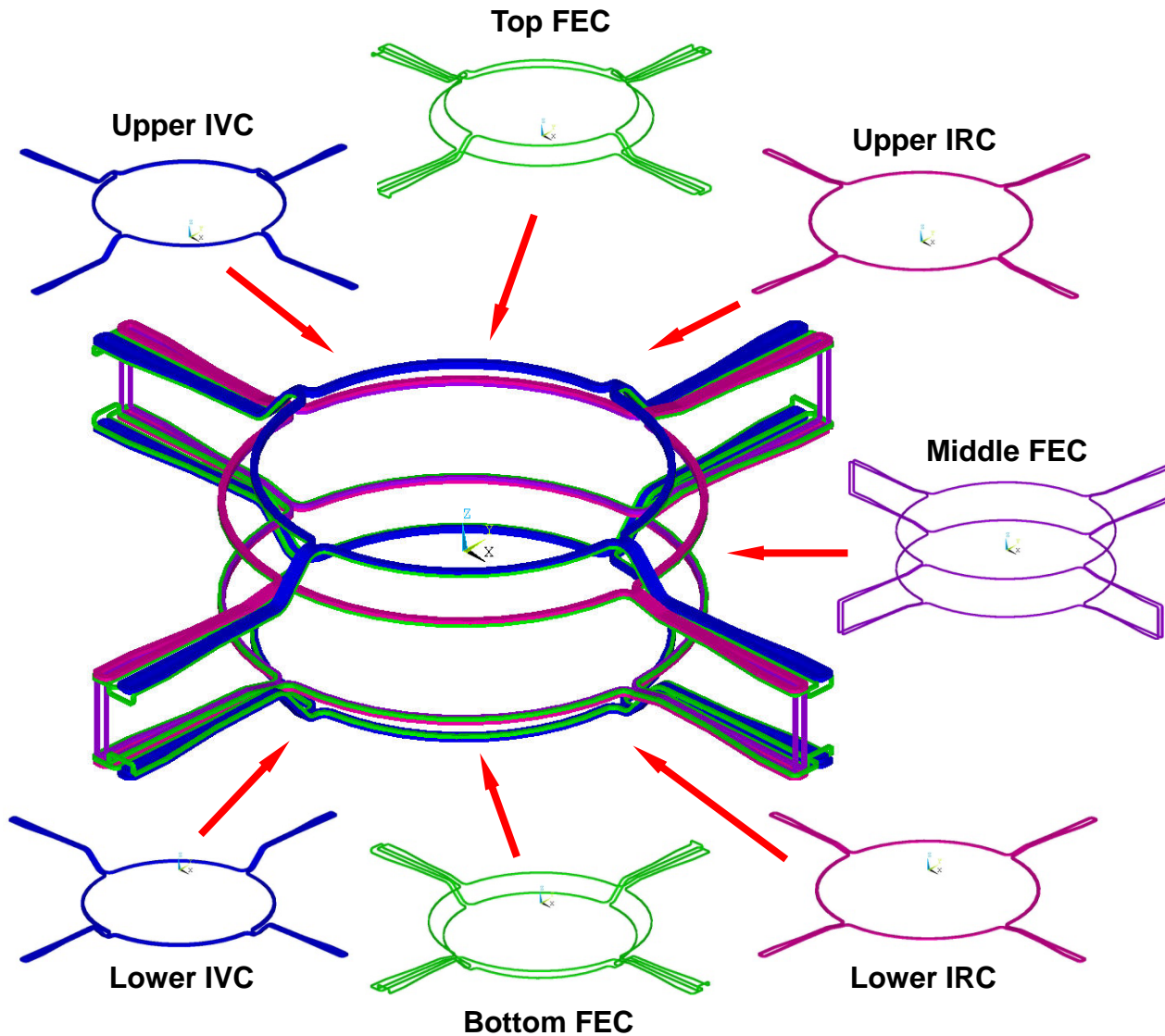
- Only even parity fulfills the Chirikov criterion for the target equilibria spanning $B_T = 2$ T and $0.8 < I_p$ (MA) < 1.1 by using the planned IVCC current in 2011

Conclusions

- ❑ Experimental equilibria of 2009-10 discharges were reconstructed using the EFIT code, including theoretically estimated vessel current and reasonable allowance for Incoloy effect.
- ❑ Equilibrium operating space much broadened in 2010 and reconstruction of achieved H-mode gave us useful guidance to understand underlying dynamics.
- ❑ Kinetic modification of MHD stability calculated by the MISK code indicates that significant rotation may be required to obtain RWM stability. Further analysis of profile variations, use of measured kinetic and rotation profiles will be made.
- ❑ A design of the passive stabilizing plates was finalized to have maximum RWM passive stabilization, and a time dependent RWM control simulation showed the mode can be stabilized with reasonable levels of feedback control power and increased power demands caused by sensor noise were also confirmed.
- ❑ The ELM mitigation potential is analyzed using the TRIP3D code, and higher m -spectrum from up-down even parity configuration would be better to obtain favorable pitch alignment for 2011 XP.

Backup Slides

Structure/Connection of KSTAR IVCC



Schematic Diagram

